Supplementary Materials

High-performance aqueous zinc-ion batteries with highly oriented MFI zeolite nanosheet separators

Haoyu Zhang[1], Sirui Chen[1], Huang Lin[1], Anding Xu[1], Xin Wen[1], Longtao Ma[2], Yu Han[1,3,4], Hui Zhang[1,3,4]

[1]School of Emergent Soft Matter, Guangdong Provincial Key Laboratory of Functional and Intelligent Hybrid Materials and Devices, South China University of Technology, Guangzhou 510640, Guangdong, China.
[2]School of Materials Science and Engineering, Guangdong Provincial Key Laboratory of Advanced Energy Storage Materials, South China University of Technology, Guangzhou 510641, Guangdong, China.
[3]Center for Electron Microscopy, South China University of Technology, Guangzhou 511442, Guangdong, China.
[4]State Key Laboratory of Pulp and Paper Engineering, South China University of Technology, Guangzhou 510640, Guangdong, China.

Correspondence to: Dr. Hui Zhang, School of Emergent Soft Matter, Guangdong Provincial Key Laboratory of Functional and Intelligent Hybrid Materials and Devices, South China University of Technology, Guangzhou 510640, Guangdong, China; Center for Electron Microscopy, South China University of Technology, Guangzhou 511442, Guangdong, China; State Key Laboratory of Pulp and Paper Engineering, South China University of Technology, Guangzhou 510640, Guangdong, China. E-mail: huizhang2023@scut.edu.cn

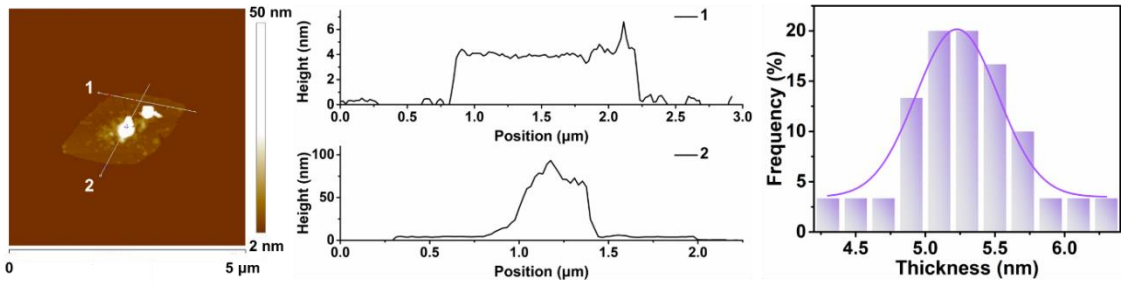

Figure S1. Thickness measurement of MFI-NS. Left: Height mapping by atomic force microscopy; Middle: Profiles along the lines marked in the left panel. Right: Thickness histogram of the peripheral regions.

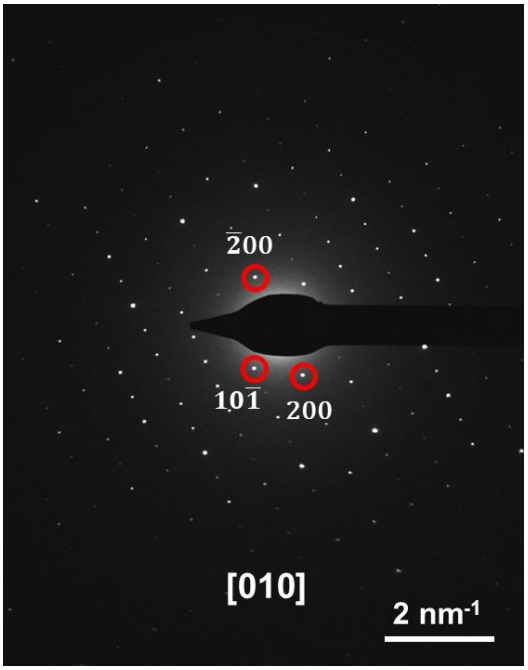

Figure S2. SAED pattern of MFI-NS. Three reflections were indexed. The zone axis is [010].

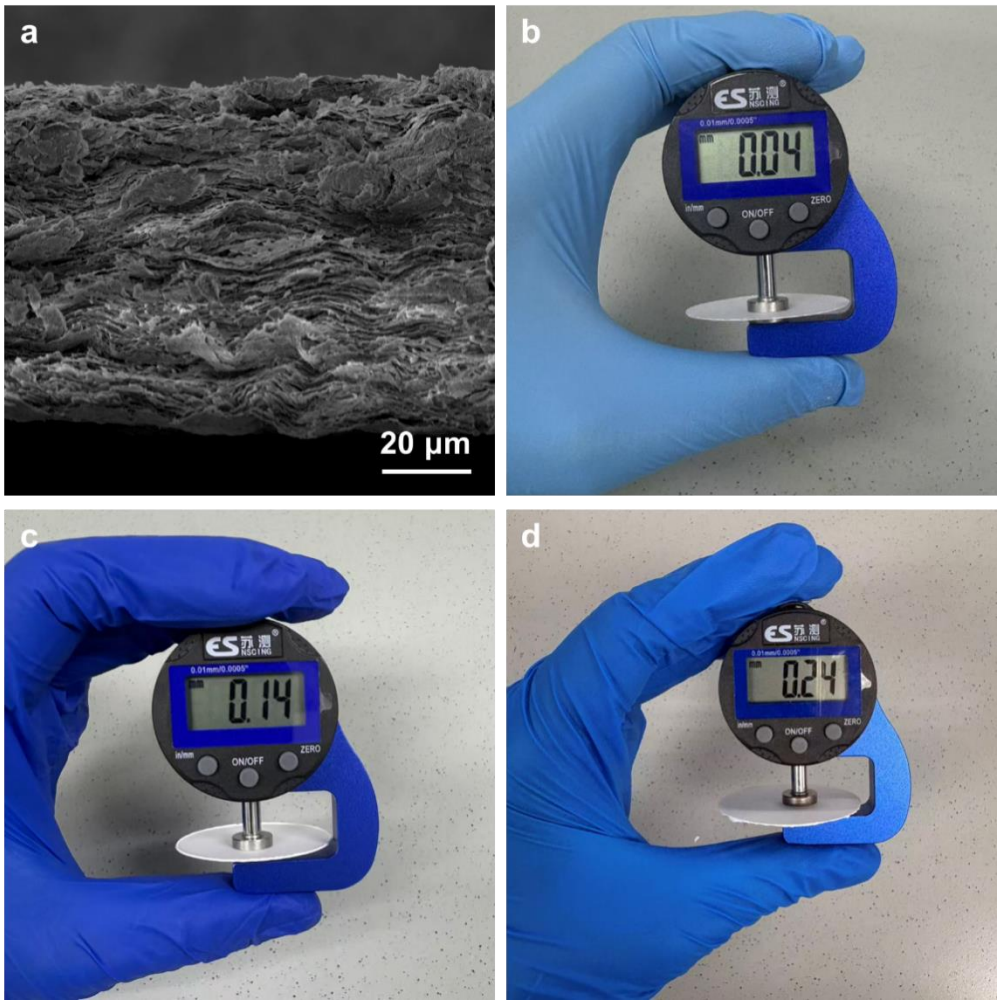

Figure S3. (a) Cross-section morphology of MFI-NS membrane. Digital photographs of (b) 40 μm, (c) 140 μm and (d) 240 μm MFI-NS membrane. Digital photographs were taken by the authors.

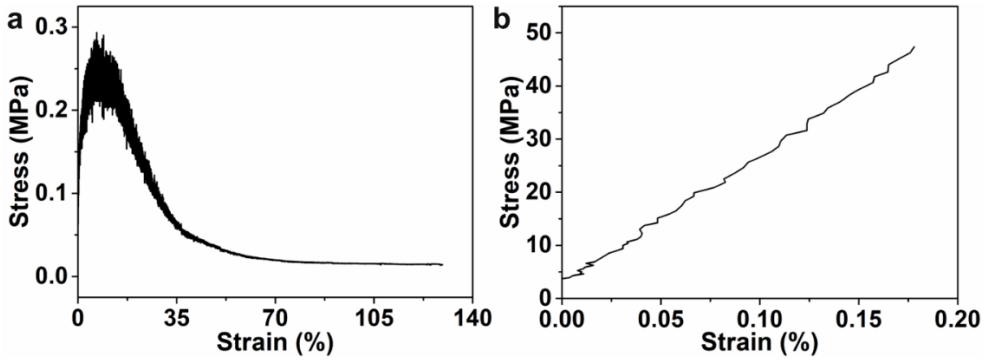

Figure S4. Tensile properties of the (a) GF and (b) MFI-NS separators. Under a tensile stress of approximately 50 MPa, the MFI-NS separator abruptly fractured.

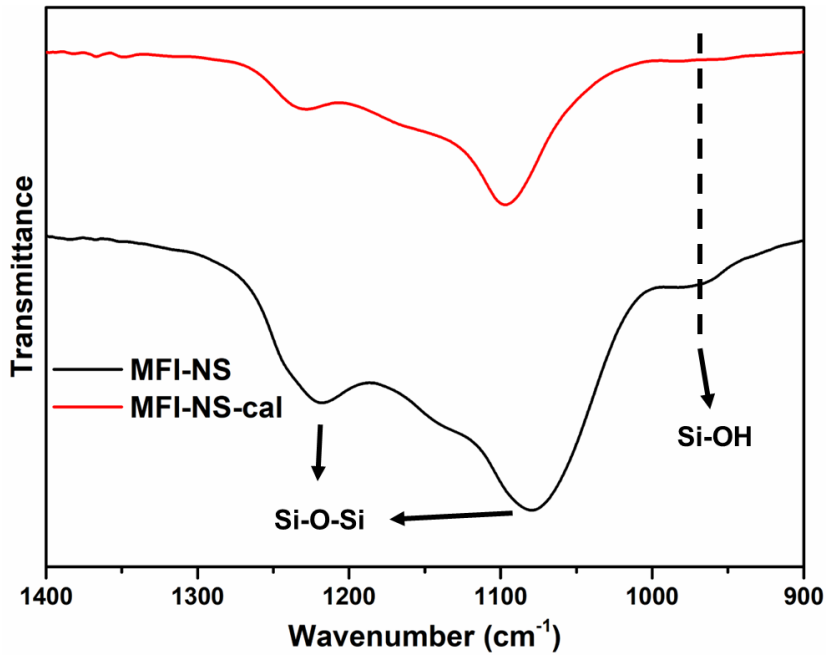

Figure S5. FT-IR spectra of MFI-NS and MFI-NS-cal. The bands at 1080 cm^{-1} and 1220 cm^{-1} result from the asymmetric stretching vibration of Si-O-Si, while the peak at 980 cm^{-1} corresponds to the Si–OH stretching vibration.

Figure S6. Contact angle of 3 M $ZnSO_4$ electrolyte on MFI-NS separators.

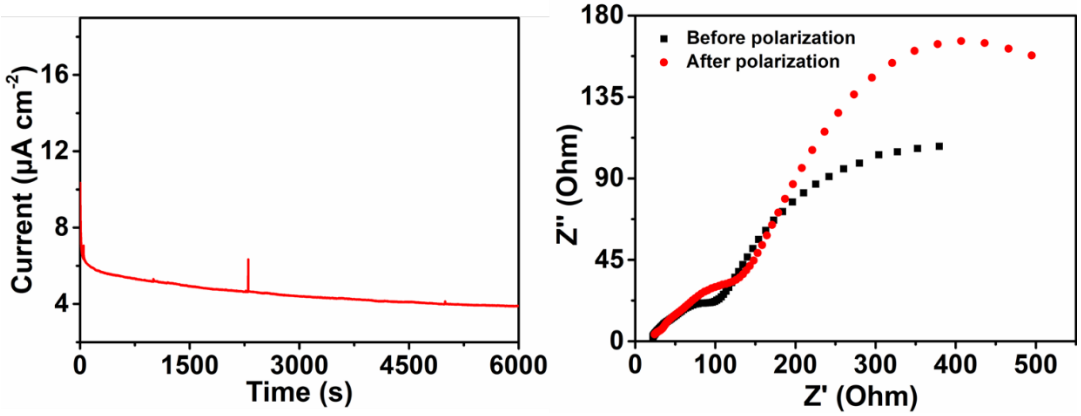

Figure S7. (a) Chronoamperometry (CA) profile of the Zn||MFI-NS||Zn symmetric cell and (b) the corresponding EIS spectra before and after the CA test.

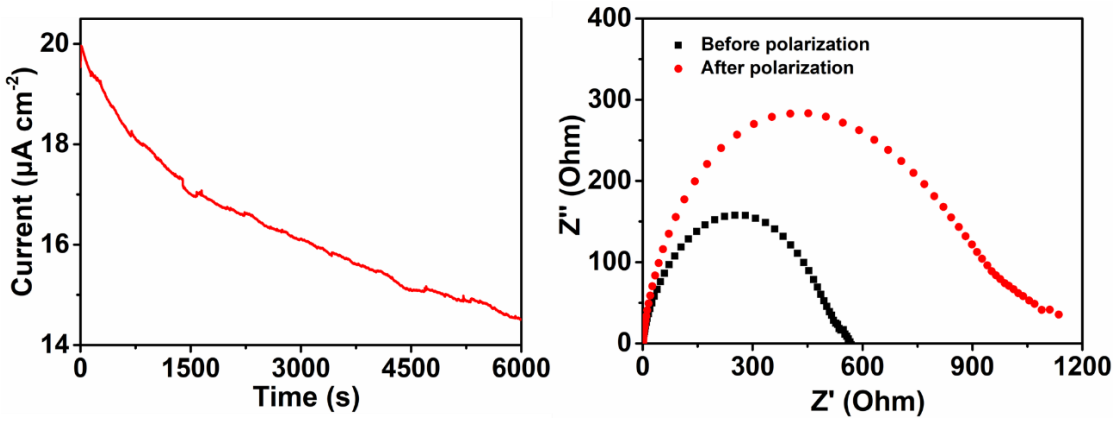

Figure S8. (a) Chronoamperometry (CA) profile of the Zn||GF||Zn symmetric cell and (b) the corresponding EIS spectra before and after the CA test.

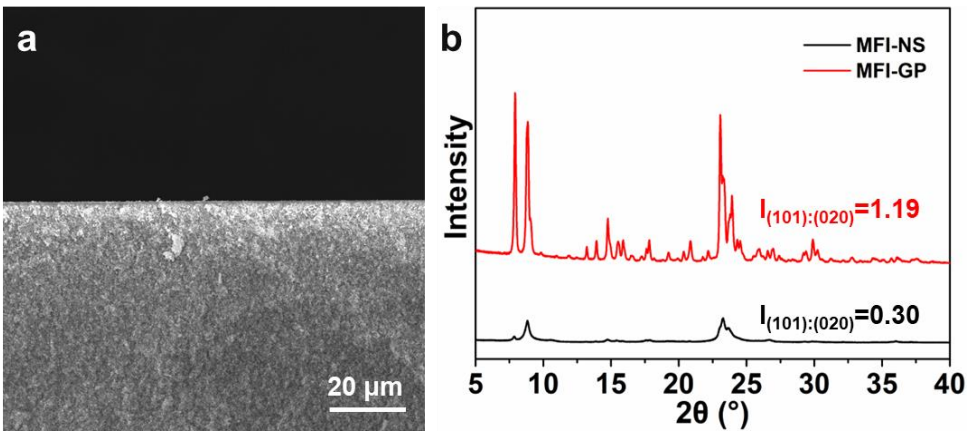

Figure S9. (a) Cross-section morphology and (b) XRD pattern of MFI-GP separator. The XRD pattern of the MFI-NS separator is provided for comparison.

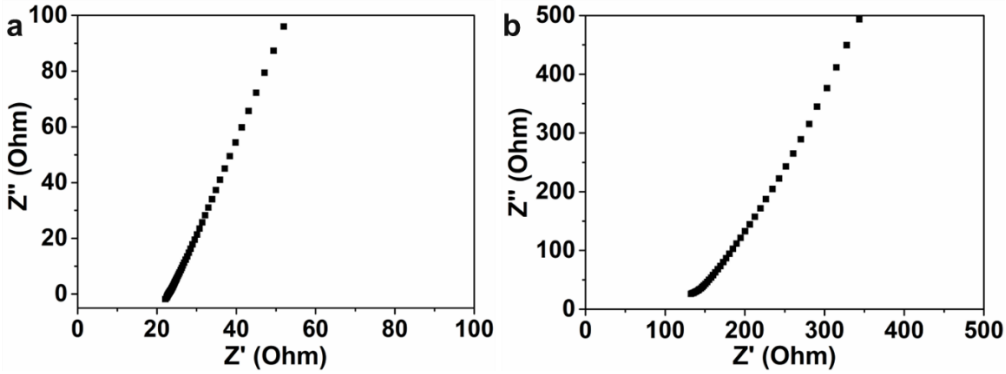

Figure S10. EIS spectra of the (a) MFI-NS and (b) MFI-GP separators.

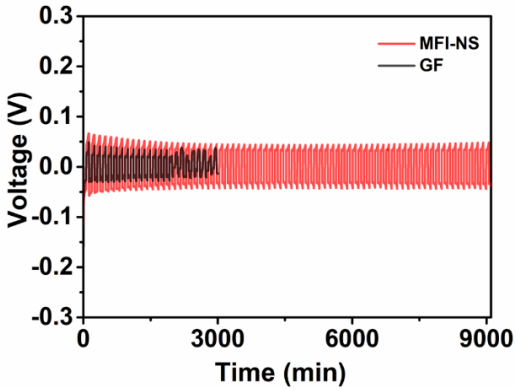

Figure S11. Long-term cycling of symmetric cells tested with 1 mA cm^{-2} and 1 mAh cm^{-2}.

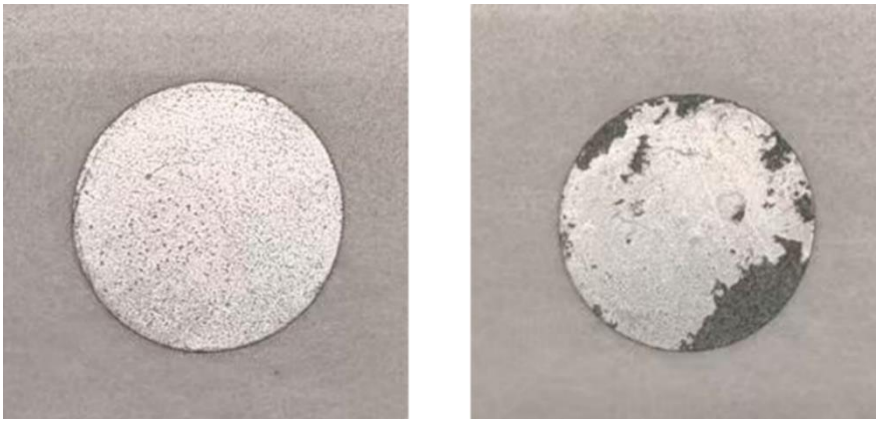

Figure S12. Digital photographs of Zn electrodes from symmetric cells with MFI-NS (left) and GF (right) separators after12000 min of cycling. Digital photographs were taken by the authors.

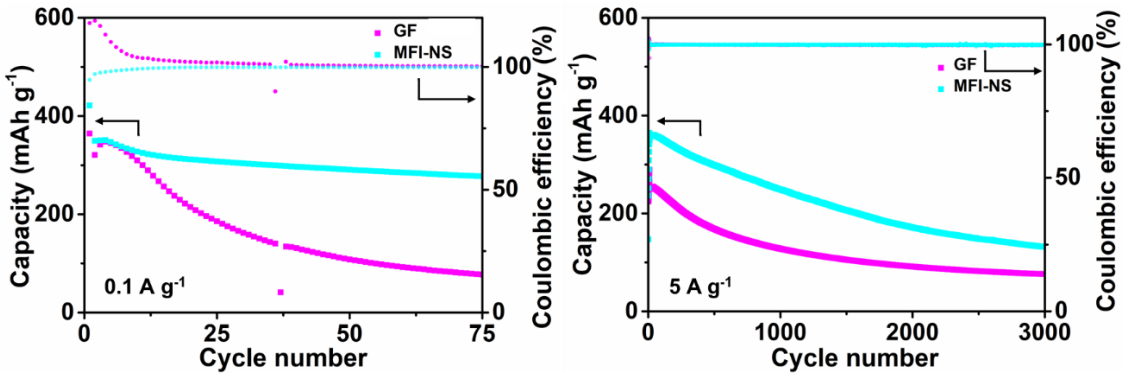

Figure S13. Long-term cycling tests of V_2O_5||MFI-NS||Zn and V_2O_5||GF||Zn cells at current densities of 0.1 A g^{-1} and 5 A g^{-1}.

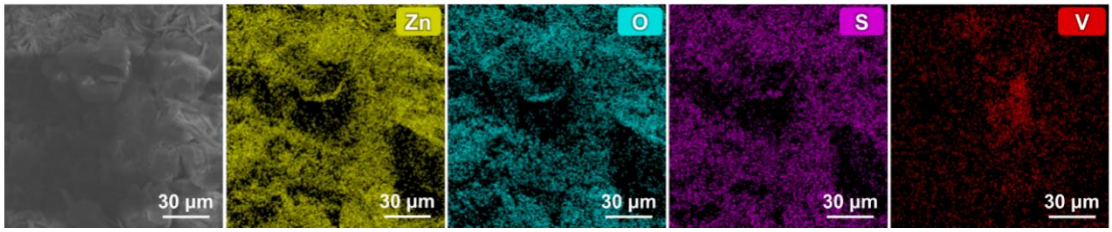

Figure S14. SEM morphology (leftmost panel) and EDS mapping of the Zn electrode after 400 cycles at 1 A g^{-1}.

Table S1. Specific surface area and porosity.

Sample	S_{BET} (m^2 g^{-1})	S_{ext} (m^2 g^{-1})	V_{total} (cm^3 g^{-1})	V_{micro} (cm^3 g^{-1})	d_p (nm)
MFI-NS-mem	66.0	51.3	0.213	0.00570	1.48
MFI-NS-mem-cal	383	171	0.434	0.110	0.590
MFI-NS-cal	429	182	0.577	0.128	0.590

Table S2. Comparison of rate performance.

Current density	This work	Ref. [1]
0.5C	432mAh g^{-1}	400 mAh g^{-1}
1C	427 mAh g^{-1}	360 mAh g^{-1}
2C	418 mAh g^{-1}	300 mAh g^{-1}
4C	396 mAh g^{-1}	270 mAh g^{-1}
8C	335 mAh g^{-1}	225 mAh g^{-1}
10C	298 mAh g^{-1}	210 mAh g^{-1}
Capacity retention from 10C to 0.5C	98.6%	96.9%

References

1. Zhu, J.; Bie, Z.; Cai, X.; et al. A Molecular-Sieve Electrolyte Membrane enables Separator-Free Zinc Batteries with Ultralong Cycle Life. *Adv. Mater.* **2022**, *34*, 2207209. https://doi.org/10.1002/adma.202207209